Springer

KSME

Journal of Mechanical Science and Technology 31 (3) (2017) 1079~1088
www.springerlink.com/content/1738-494x(Print)/1976-3824(Online)
DOI 10.1007/s12206-017-0207-0

Effects of gear modifications on the dynamic characteristics of wind turbine gearbox considering elastic support of the gearbox †

Shuaishuai Wang[1], Caichao Zhu[1,*], Chaosheng Song[1], Huachao Liu[1], Jianjun Tan[1] and Houyi Bai[2]

[1]*The State Key Laboratory of Mechanical Transmissions, Chongqing University, Chongqing, 400030, China*
[2]*Chongqing Wangjiang Industrial Co., Ltd., Chongqing, 400081, China*

(Manuscript Received July 30, 2016; Revised November 19, 2016; Accepted November 23, 2016)

Abstract

The reliability and service life of wind turbines are directly influenced by the dynamic performance of the gearbox under the time-varying wind loads. The control of vibration behavior is essential for the achievement of a 20-year service life. We developed a rigid-flexible coupled dynamic model for a wind turbine gearbox. The planet carrier, the housing, and the bedplate are modelled as flexibilities while other components are assumed as rigid bodies. The actual three points elastic supporting are considered and a strip based mesh model is used to represent the engagement of the gear pairs. The effects of gear tooth modifications on the dynamics were investigated. Finally, we conducted a dynamic test for the wind turbine gearbox in the wind field. Results showed that the contact characteristics of gear pairs were improved significantly; the peak-to-peak value of transmission error of each gear pair was reduced; the amplitudes of the vibration acceleration and the structural noise of the wind turbine gearbox were lowered after suitable tooth modification.

Keywords: Wind turbine gearbox; Elastic supporting; Gear modification; Dynamic characteristics; Experiments

1. Introduction

The rapid development of the global wind energy market in recent years has fueled significant growth in the power output of the wind turbine. Since the wind turbine gearbox is installed in the narrow space of a nacelle on top of a high tower, it has the highest failure rate due to the varying and random wind loads [1]. The reliability and durability of wind turbine gearboxes has attracted more and more attention. Gear modification can reduce the gear meshing impact and improve load distribution performance. Meanwhile, it is helpful to decrease the vibration and noise.

In recent years, several studies have been conducted on the vibration and noise behaviors of wind turbine drive trains. Using the flexible multibody modeling technique, the reliability, noise and vibration behavior based on three different configurations (threepoint mounting, double bearing configuration, and hydraulic damper system) were investigated by Helsen et al. [2]. They illustrated that different suspension methods and variation of support parameters had a great influence on the dynamic performance of the gearbox. In addition, they studied gearbox modal behaviors using three different models: The purely torsional, rigid six degree of freedom with discrete flexibility and flexible multibody technique [3]. Park et al. [4] developed a 1.5 MW wind turbine gearbox dynamic model considering the flexibilities of housing, planet carriers and ring gears, the nonlinear mesh stiffness of gears and the nonlinear stiffness of bearings. Then, the effects of helix modification on tooth surface load distribution and load sharing were analyzed. Ma et al. [5] developed a mesh stiffness model for profile shifted gears with addendum modifications and tooth profile modifications and determined the optimum modification curves under different tooth profile modifications. A finite element based dynamic model of high speed gear-rotor-bearing system was developed by Hu et al. [6] and the effects of tooth profile modification on dynamic responses were studied. Parker et al. [7] developed a nonlinear analytical model considering the dynamic load distribution between individual gear teeth, the time-varying mesh stiffness, profile modifications and contact loss. Then, the effects of tooth profile modification on multi-mesh gear set vibration were studied. Yu et al. [8] proposed a new theory called compensated conjugation for gear conjugation and PPTE reduction. They offered a very general criterion for proper modification rather than being limited to a certain type of modification or geometry. Wu et al. [9] used a finite element analysis software ANSYS to analyze the gear tooth deformation on influence of gear meshing transmission performance. Velex et al. [10] used a modular three-dimensional model of multi-mesh gears to analyze theo-

*Corresponding author. Tel.: +86 23 65111192, Fax.: +86 23 65111192
E-mail address: cczhu@cqu.edu.cn
† Recommended by Associate Editor Eung-Soo Shin

retically the link between dynamic mesh excitations and transmission errors. Li et al. [11] investigated the effects of tooth profile modification and lead relieving on tooth engagements of a pair of spur gears and the effects of misalignment error of gear shafts on the plane of action, tooth lead crowing and transmitted torque on tooth mesh stiffness. Bahk et al. [12] developed an analytical tooth profile modification model for planetary gears, and evaluated its accuracy for dynamic analysis by comparisons with a benchmark finite element analysis. Zhu et al. [13, 14] developed a dynamic model of a wind turbine gearbox with flexible pins and investigated the effect of such pins on the dynamic behavior of wind turbine planetary gear drives. A drive train model of wind turbine was also established and the dynamic characteristics based on the measured load spectrum were investigated by them. Petković et al. [15, 16] proposed a wind generator equipped with CVT, and proposed the application of Adaptive neuro-fuzzy inference system (ANFIS) to control the CVT ratio to extract the maximal wind energy through the wind turbine. In addition, they adapted the ANFIS to estimate optimal coefficient value of the wind turbines. Shamshirband et al. [17, 18] presented a Support vector regression (SVR) technique to estimate the wind turbine power coefficient and to predict the optimal values of the wind turbine reaction torque. The results showed that an improvement in predictive accuracy and capability of generalization can be achieved by the SVR approach. Nikolic et al. [19] established an adaptive neuro-fuzzy method for the estimation of wind turbine rotor performances, power output, torque output and rotor rotational speed in regard to diffuser effect and wind input speed. Wan et al. [20, 21] performed a systematic study to comprehensively model the ploughing mechanism in the milling process, and the ploughing mechanism was modeled in a generalized way to be suitable for predicting both static and dynamic cuts. They also studied the stability lobe prediction methods for the milling process with multiple delays, and highlighted the influences of different cutting force models on stability lobes. However, little work has been conducted on the effects of gear tooth modifications on the dynamic performance of wind turbine gearbox considering the actual three points elastic supporting of the gearbox with the actual measured wind load spectrum and the related experimental verification.

2. Transmission principles and dynamic modeling of the wind turbine transmission system

2.1 Transmission principles

The selected wind turbine gearbox consists of a planetary stage and two parallel stages with an overall transmission ratio of 1:115.25. The basic structure of the gear transmission system is shown in Fig. 1. For the first stage, power is transmitted to the carrier through the blades, rotor and main shaft and then transmitted to the sun gear via planets and ring. For the second stage, the power is transmitted to the middle stage gear pair (g1-g2) by sun gear before it's finally delivered to the high-speed shaft through the high-speed gear pair (g3-g4). As shown in Fig. 1, the symbols v, T_{in} and T_{out} represent the wind speed, the input torque, and the output torque, respectively. The detailed parameters of the transmission system are listed in Table 1.

Table 1. The geometric parameters of wind turbine gear transmission system.

Stage	Item	Ring gear	Sun gear	Planet gear
1st	Number of teeth	96	21	96
	Module (mm)	15	15	15
	Pressure angle (°)	25	25	25
	Helix angle (°)	8	8	8
	Item	Wheel		Pinion
2nd	Number of teeth	97		23
	Module (mm)	11		11
	Pressure angle (°)	20		20
	Helix angle (°)	10		10
3rd	Number of teeth	103		21
	Module (mm)	8		8
	Pressure angle (°)	20		20
	Helix angle (°)	10		10

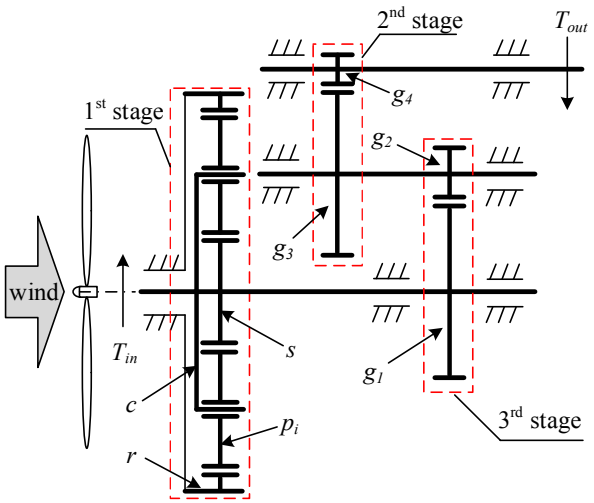

Note: r- the internal ring; c- the carrier; p_i- the planet gears; s- the sun gear; g_1 and g_2- the wheel and the gear of the intermediate gear stage, respectively; g_3 and g_4- the wheel and the gear of the high-speed gear stage, respectively.

Fig. 1. The diagram of transmission principle of wind turbine transmission.

2.2 Dynamic modeling

The wind turbine gearbox used in this study is a conventional gearbox for a 2200 KW wind turbine system. The main components of the wind turbine transmission system are the hub, the main shaft, the gearbox, and the generator. The wind

turbine transmission system applies a three-point supporting configuration, where the main shaft is supported by a main bearing and the gearbox is connected to the nacelle by means of torque arms. Important components of the system are shown in Fig. 2 and the symbols in Fig. 2 are described in Table 2 [2].

The flexibility of the bearing is very important for the wind turbine drive train [3, 22]. Bearings are usually modelled in a discrete fashion by means of stiffness and damping relationships [23]. However, this approach neglects the off-diagonal stiffness terms in the bearing stiffness matrix. This is because it does not consider the coupling effects between the different degrees of freedom, which has a great influence on the dynamic behaviors on the system [24]. Considering all off-diagonal cross stiffness terms, the stiffness matrix of the bearings in the gearbox and main bearing in this study can be represented by

$$K_{bearing}=\begin{bmatrix} K_{xx} & K_{xy} & K_{xz} & K_{xu} & K_{xv} & 0 \\ K_{yx} & K_{yy} & K_{yz} & K_{yu} & K_{yv} & 0 \\ K_{zx} & K_{zy} & K_{zz} & K_{zu} & K_{zv} & 0 \\ K_{ux} & K_{uy} & K_{uz} & K_{uu} & K_{uv} & 0 \\ K_{vx} & K_{vy} & K_{vz} & K_{vu} & K_{vv} & 0 \\ 0 & 0 & 0 & 0 & 0 & 0 \end{bmatrix}. \quad (1)$$

The bushing element for the torque arm can be represented by a single 6×6 spring-damping relation and only the diagonal terms were considered.

$$K_{bushing}=\begin{bmatrix} K_x & 0 & 0 & 0 & 0 & 0 \\ 0 & K_y & 0 & 0 & 0 & 0 \\ 0 & 0 & K_z & 0 & 0 & 0 \\ 0 & 0 & 0 & K_u & 0 & 0 \\ 0 & 0 & 0 & 0 & K_v & 0 \\ 0 & 0 & 0 & 0 & 0 & K_w \end{bmatrix}, \quad (2)$$

where x, y and z represent the three translational degrees of freedom. u, v and w represent the three rotational degrees of freedom around x axes, y axes and z axes, respectively.

Gear mesh stiffness is traditionally represented by a single spring element along the line of action. However, this method cannot consider the variation of tooth surface pressure along the direction of tooth width. To analyze the gear contact more accurately, we used a strip-based mesh model as shown in Fig. 3. It assumes that each gear is divided into several strips across the contact line [25, 26]. Then the stiffness between each pair of strips of the pinion and gear is calculated by the ISO 6336 [27]. Then, the synthesized mesh stiffness for the gear pair can be obtained.

All structural components are considered to be rigid except for the planet carrier, housing and bedplate. These three components are represented by finite element models. Then the finite element models are condensed to the reduced stiffness matrices and are coupled with the transmission system components through interface nodes. The rigid-flexible coupled multi-body dynamic model has been developed using the commercial software Masta [28], as shown in Fig. 4.

Table 2. Symbols in the topological graph of the wind turbine drive train.

Symbols	Meaning	Symbols	Meaning
R	Rotor	MB	Main shaft bearing bearing
S	Shaft	B	Bushing
GR	Generator	CP	Coupling
G	Outer gear	P	Planet gear
SG	Sun gear	C	Carrier
GB	Gearbox		

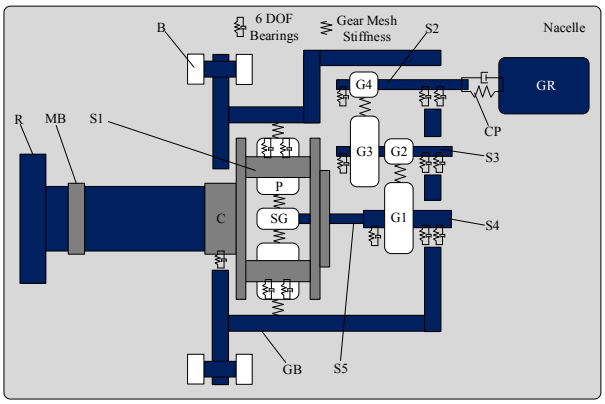

Fig. 2. Topological graph of the wind turbine drive train.

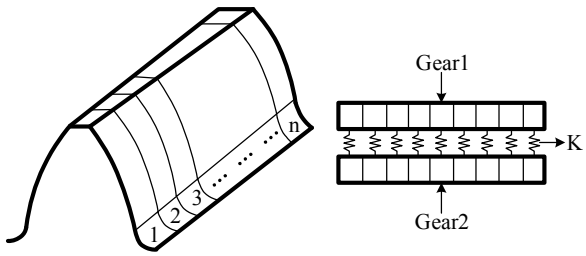

Fig. 3. The slices model of gear.

3. Gear tooth modifications and tooth contact analysis

Suitable gear tooth modification can improve the tooth contact performance and further decrease the vibration and structural noise of the wind turbine transmission system effectively. To perform gear tooth modification effectively in most working conditions, it is essential to consider the actual load spectrum for the gear tooth modification. A real-time load test was conducted to capture the time-history of the wind load within a period and the time-history load can be condensed to obtain a load spectrum as shown in Fig. 5.

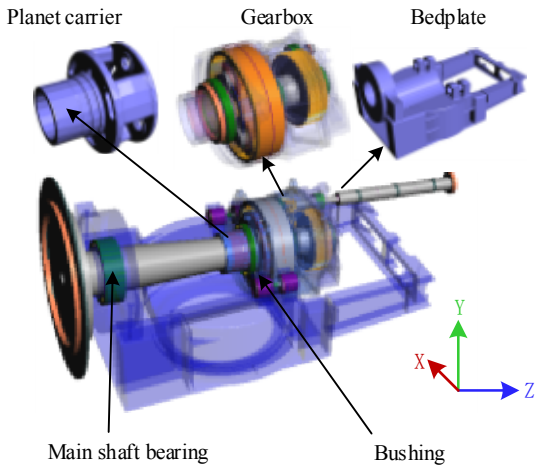

Fig. 4. Dynamic model of the wind turbine transmission system.

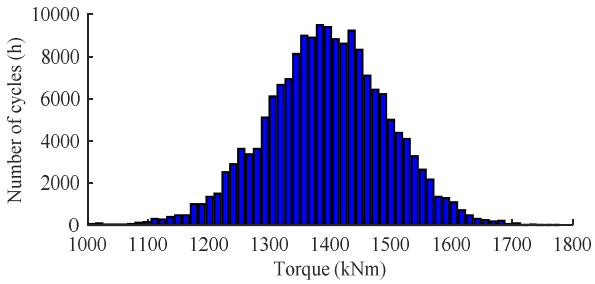

Fig. 5. Load spectrum of megawatt level wind turbine gearbox.

First, tooth modification is optimized automatically by the commercial software Masta according to the measured load spectrum. The optimization target for gear modification is the contact stress, and the max contact stress can be represented by Eq. (3). The initial relief amount can be determined by the $\sigma_{\sum \min}$.

$$\sigma_{\sum} = k_1\sigma_1 + k_2\sigma_2 + \cdots + k_n\sigma_n \,, \tag{3}$$

where k_n is the weight ratio of the n-th condition of the load spectrum ($k_1 = k_2 = \cdots = k_n$), and σ_n (MPa) is the maximum tooth surface contact stress of the n-th condition in load spectrum.

For the automatic tooth modification, the combined lead and profile modifications are used. For lead modification, it contains crowning modification, helix angle modification and gear flank end modification. For the profile modification, it contains barreling modification, pressure angle modification, gear tip and gear root modification. Then, the contact pattern, contact pressure and the transmission error are analyzed. Based on the analysis results, the tooth modification parameters are manually adjusted to make the contact pattern larger and transmission error lower. The final relief amount of each gear pair can be seen in Figs. 6-8.

The calculated contact patterns with and without gear tooth modification under rating condition are shown in Figs. 9-11.

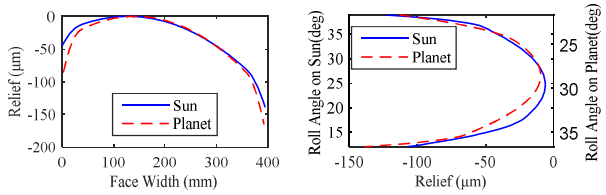

Fig. 6. Relief of the planetary gear pair (Sun-planet).

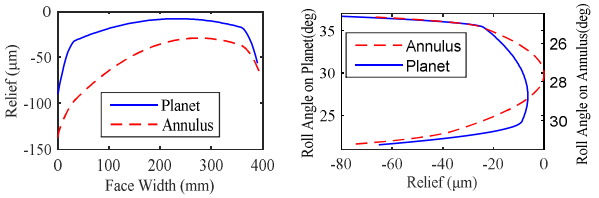

Fig. 7. Relief of the planetary gear pair (Annulus-planet).

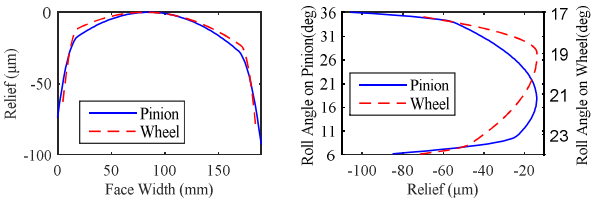

Fig. 8. Relief of the high-speed stage gear pair.

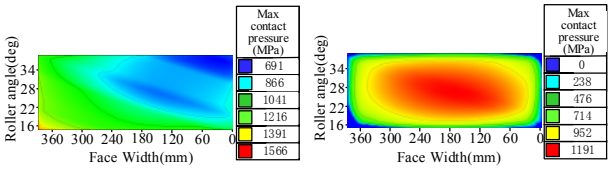

Fig. 9. Contact patterns of sun-planet meshes.

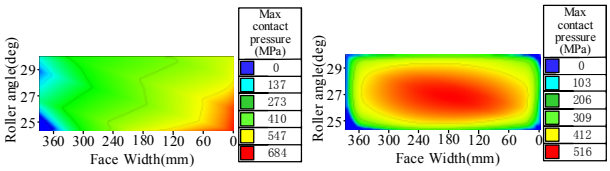

Fig. 10. Contact patterns of annulus-planet meshes.

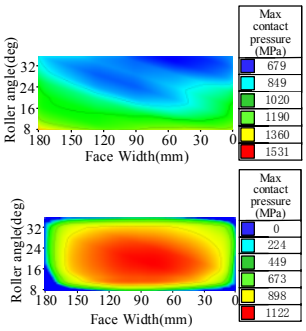

Fig. 11. Contact patterns of pinion-wheel meshes of high-speed stage.

Table 3. Max contact pressure value with/without modification.

Max contact pressure (Mpa)	SP	AP	WP (2nd)	WP (3rd)
Without modification	1566	684	1750	1531
With modification	1191	516	1265	1122
Percentage reduction	23.95 %	24.56 %	27.71 %	26.71 %

Note: SP- Planet-sun gear pair; AP- Annulus-planet gear pair; WP- Wheel-pinion gear pair.

Table 4. Face load factor with/without modification.

Face load factor	SP	AP	WP (2nd)	WP (3rd)
Without modification	1.6252	1.7059	1.4726	1.4357
With modification	1.3150	1.2786	1.2819	1.2744
Percentage reduction	19.09 %	25.05 %	12.95 %	11.23 %

The maximum contact pressure value and face load factor for each gear pair with and without modification can be seen in Tables 3 and 4, respectively. According to the results, when the modification is applied, the maximum load zone on the contact pattern shifts to the center of tooth surface, the edge contact originally seen in the gear tooth surface disappears, the distribution of loads on the tooth surface becomes uniform, and the maximum contact stress and face load factor of the tooth surface decrease for each gear pair.

Generally, Transmission error (TE) is considered to be the main source of noise and vibration of gear transmission system. The calculated time-varying transmission error of gear pairs with and without modifications is shown in Fig. 12. The peak-peak values of the transmission error are listed in Table 5. It can be seen that the peak-to-peak value of TE for each gear pair and system is reduced significantly due to gear tooth modification.

4. Dynamics analysis of the wind turbine gearbox

Using the proposed coupled drive train dynamic model, the dynamic responses are computed and analyzed subsequently. The acceleration response of high-speed stage bearing housing for the down wind direction is studied under the rating condition. Fig. 13 illustrates the dynamic response at the measured point. The excitation frequencies (i.e., meshing frequencies of gear pairs and their harmonics) under rating condition are listed in Table 6.

From the results shown in Fig. 13, the peak values of acceleration response corresponding to the first order and second order meshing frequencies of the high-speed stage are larger than others without modification. In addition, their reduction corresponding to the two typical frequencies is also larger than others with and without modification. It illustrates that the excitations from the two typical frequencies can produce a greater impact on the dynamic behavior of the gearbox. The maximum vibration acceleration values at the mentioned measured point excited by the two typical frequencies can be seen in Table 7.

Table 5. Peak-to-peak value of TE with/without modification.

Peak-to-peak value (μm)	SP	AP	WP (2nd)
Without modification	16.186	17.675	12.898
With modification	8.961	6.946	5.259
Percentage reduction	44.637 %	60.702 %	59.226 %
Peak-to-peak value (μm)	WP(3rd)	System (mRad)	
Without modification	7.317	6.25	
With modification	3.726	2.18	
Percentage reduction	49.077 %	65.120 %	

Table 6. Excitation frequencies under rating condition.

Generator speed (r/min)		1830	
Excitation frequencies (kHz)	LM_1p	LM_2p	LM_3p
	0.0309	0.0618	0.0927
Excitation frequencies (kHz)	IM_1p	IM_2p	IM_3p
	0.143	0.286	0.429
Excitation frequencies (kHz)	HM_1p	HM_2p	HM_3p
	0.6405	1.281	1.9215

Note: LM_ip- meshing frequency of the low-speed stage; IM_ip- meshing frequency of the intermediate-speed stage; HM_ip- meshing frequency of the high-speed stage. i = 1 for lst order, i = 2 for 2nd order and i = 3 for the 3rd order.

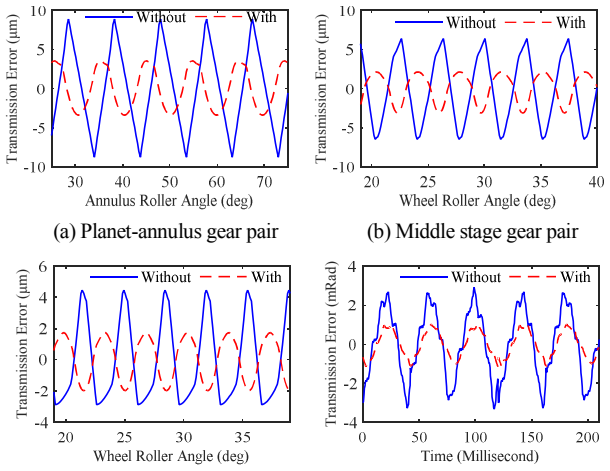

(a) Planet-annulus gear pair (b) Middle stage gear pair

(c) High speed stage gear pair (d) System transmission error

Fig. 12. Transmission error of each gear pairs and system.

To reflect the effect of the tooth modification on the dynamics of the gearbox more accurately, it is necessary to analyze the acceleration response at the measured point within the whole operation range. The excitation frequencies HM_1p and HM_2p are displayed in Table 8 and the results are shown in Fig. 14. The maximum acceleration of three orthotropic directions at the measured point with and without modification is listed in Table 9. According to the results shown in Fig. 14 and Table 9, the amplitudes of acceleration at three orthotropic directions are reduced within a large speed range with tooth modification. However, the extent of the reduction

Table 7. Maximum acceleration (m/s^2) at high-speed bearing housing in downwind direction under the rating condition.

Directions and frequencies	X		Y	
	HM_1p	HM_2p	HM_1p	HM_2p
Without modification	2.86	4.12	1.73	1.38
With modification	1.59	0.79	0.96	0.27
Reduction percentage	44.4 %	80.8 %	44.5 %	80.4 %
Directions and frequencies	Z			
	HM_1p	HM_2p		
Without modification	3.26	2.80		
With modification	1.81	0.54		
Reduction percentage	44.5 %	80.7 %		

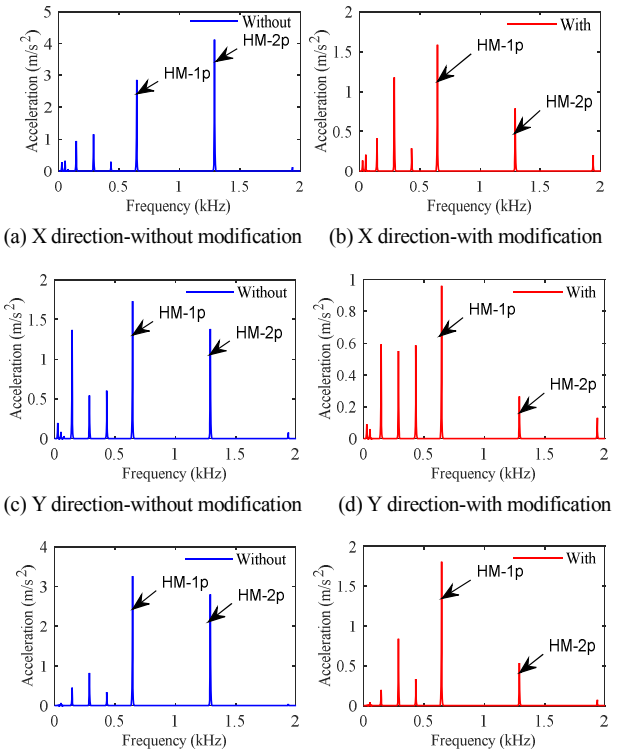

(a) X direction-without modification (b) X direction-with modification

(c) Y direction-without modification (d) Y direction-with modification

(e) Z direction-without modification (f) Z direction-with modification

Fig. 13. The vibration acceleration response of high-speed shaft bearing housing of down wind direction with and without modification.

is different under different excitation frequencies. Compared with the reduction amount of first-order acceleration response, larger amount of decrease can be noticed for the second order. The reduction percentages of first-order acceleration response at three orthotropic directions are 44.7 % approximately, while it reaches about 80.5 % for the second order. It indicates that dynamic performance of the gearbox has been improved significantly.

The structural noise caused by vibration is the main source of the radiation noise of the gearbox. The vibration acceleration response histories shown in Fig. 14 were processed by 1/3 multiple frequency, and then, the structural noises at the measured point were acquired within the working speed range

Table 8. Excitation frequencies under different rotational speeds.

Different speed (r/min)	Cut-in speed	Cut-out speed
	1050	1900
HM_1p (kHz)	0.3675	0.665
HM_2p (kHz)	0.735	1.330

Table 9. Maximum acceleration value (m/s^2) at high-speed bearing housing in downwind direction within a large speed range.

Directions and frequencies	X		Y	
	HM_1p	HM_2p	HM_1p	HM_2p
Without modification	7.52	4.31	4.39	7.56
With modification	4.16	0.84	2.42	1.47
Reduction percentage	44.7 %	80.5 %	44.9 %	80.6 %
Directions and frequencies	Z			
	HM_1p	HM_2p		
Without modification	3.98	5.86		
With modification	2.21	1.14		
Reduction percentage	44.5 %	80.5 %		

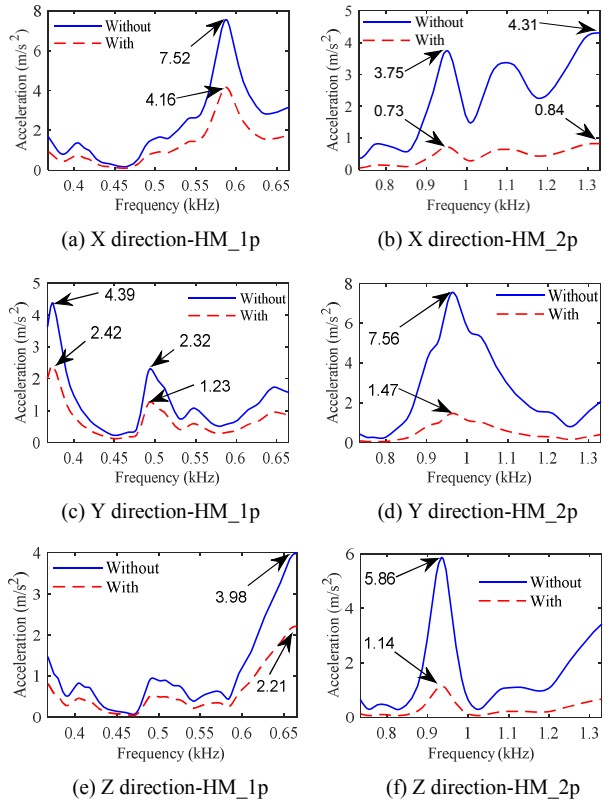

(a) X direction-HM_1p (b) X direction-HM_2p

(c) Y direction-HM_1p (d) Y direction-HM_2p

(e) Z direction-HM_1p (f) Z direction-HM_2p

Fig. 14. The vibration acceleration response within a large speed range with and without modification.

by Eq. (4), as shown in Fig. 15.

$$L_a = 10\log\frac{a^2}{a_0^2} = 20\log\frac{a}{a_0}, \quad (4)$$

Table 10. Maximum structural noise (dB) at high-speed bearing housing in downwind direction within a large speed range.

Directions and frequencies	X		Y	
	HM_1p	HM_2p	HM_1p	HM_2p
Without modification	137.8	131.4	127.0	137.6
With modification	132.4	117.2	122.1	123.3
Reduction percentage	3.92 %	10.81 %	3.86 %	10.39 %
Directions and frequencies	Z			
	HM_1p	HM_2p		
Without modification	120.0	135.3		
With modification	114.4	121.2		
Reduction percentage	4.67 %	10.50 %		

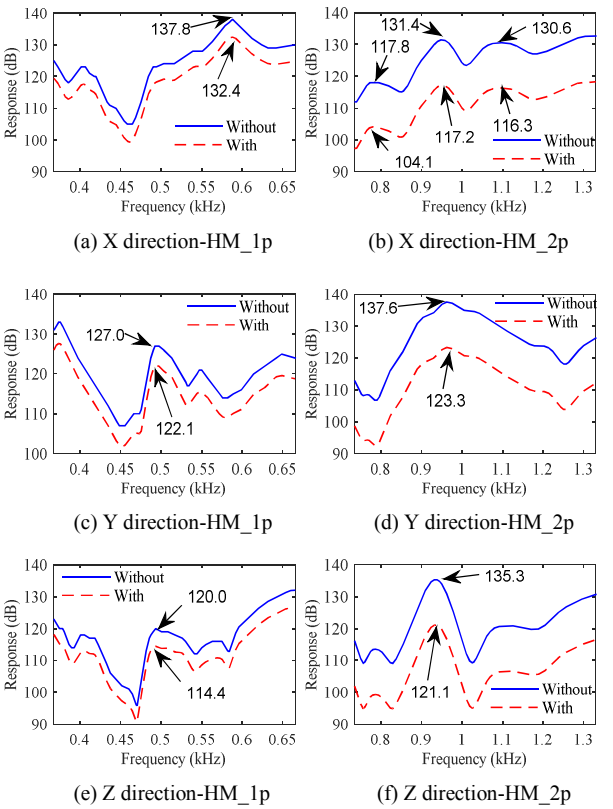

(a) X direction-HM_1p (b) X direction-HM_2p

(c) Y direction-HM_1p (d) Y direction-HM_2p

(e) Z direction-HM_1p (f) Z direction-HM_2p

Fig. 15. The structural noise response within a large speed range with and without modification.

where La-1/3 harmonic structure noise of acceleration level, unit (dB); a- the effective value of the acceleration in a frequency band that taking a certain frequency as the center frequency, unit (m/s^2); a0- datum acceleration, a0=10^{-6} m/s^2.

From the results in Fig. 15, the structural noise of first-order and second-order at the measured point are reduced with modification. The maximum values of structural noise at the three orthotropic directions within the whole working range are listed in Table 10. It indicates that the maximum structural noise of first-order is reduced by 5 dB approximately, and the reduction percentage is about 4 % with modification. However, the reduction of second-order is higher than the first-order and it reaches 10.5 %.

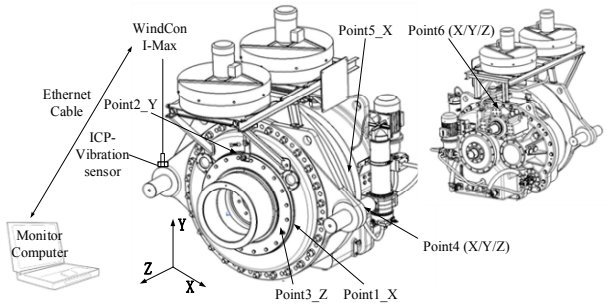

Fig. 16. Diagram of the experimental measurement system and arrangement of measuring points.

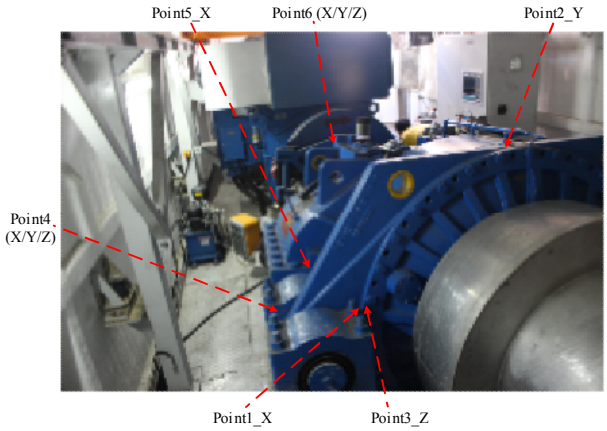

Fig. 17. Locations of the measuring points in the test field.

5. Vibration test of the wind turbine gearbox

To verify the simulated results, We did a vibration test of the actual gearbox. The measurement system and the arrangement of measuring points corresponding to the test are shown in Fig. 16. A real-time measurement system was developed using WindCon [29], which is a condition monitoring system designed by SKF for wind turbines. The vibration signals were collected through the sensors installed on the bearing housings of some key components of gearbox, such as torque arms, ring, low-speed shaft and high-speed shaft and so on. Then, the collected data was transmitted to the computer by Ethernet cable for the online monitoring and data processing. The locations of the measuring points in the test field are shown in Fig. 17.

To verify the simulation results convincingly, a rated working condition was selected – with the speed of the high-speed shaft being 1830 r/min and the generator power being 2200 kw, which is consistent with the working condition applied in the simulation model. The detailed excitation frequencies on the working condition can be viewed through the Table 6.

The vibration accelerations in time-domain and the frequency-domain of the high-speed shaft bearing housing in

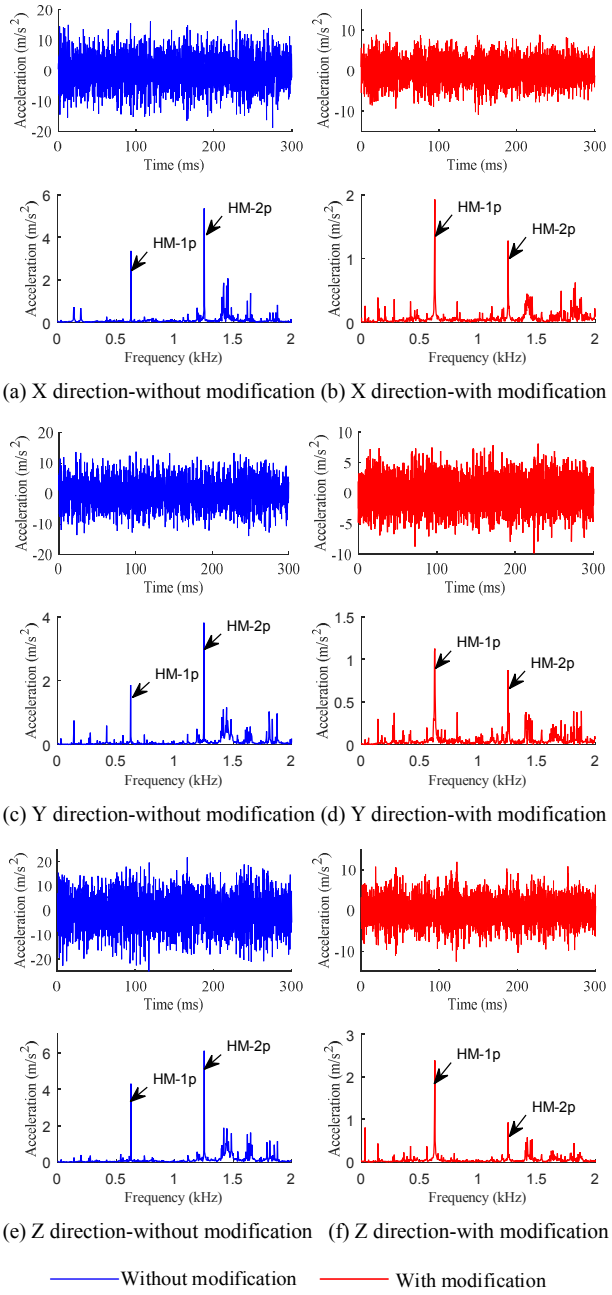

Fig. 18. The time-domain and frequency-domain acceleration response at the high-speed bearing housing in downwind direction under rating condition.

downwind direction with and without gear modification are shown in Fig. 18. From the results, the main frequency components of the accelerations are the high-speed mesh frequency and its second-harmonic. It indicates that the first-order and second-order mesh frequencies of high-speed stage have great contribution to the response of the measured point. The peak values of the first- and second-order acceleration response at three orthotropic directions with and without gear modification are listed in Table 11. It indicates that the reduction of the first-order acceleration response peak is less than

Table 11. Maximum acceleration (m/s^2) at high-speed bearing housing in downwind direction under the rating condition.

Directions and frequencies	X		Y	
	HM_1p	HM_2p	HM_1p	HM_2p
Without modification	3.355	5.361	1.869	3.821
With modification	1.927	1.277	1.128	0.878
Reduction percentage	42.6 %	76.2 %	39.6 %	77.0 %
Directions and frequencies	Z			
	HM_1p	HM_2p		
Without modification	4.301	6.111		
With modification	2.394	0.935		
Reduction percentage	44.3 %	84.7 %		

Table 12. The comparison of the simulation results in Table 7 and the experiments results in Table 11.

Directions and frequencies	X		Y	
	HM_1p	HM_2p	HM_1p	HM_2p
Simulation results	44.4 %	80.8 %	44.5 %	80.4 %
Experiments results	42.6 %	76.2 %	39.6 %	77.0 %
Percentage deviation	4.1 %	5.7 %	11.0 %	4.2 %
Directions and frequencies	Z			
	HM_1p	HM_2p		
Simulation results	44.5 %	80.7 %		
Experiments results	44.3 %	84.7 %		
Percentage deviation	0.4 %	4.7 %		

Note: The simulation results and experimental results are corresponding to the reduction percentage in Tables 7 and 11, respectively.

the second-order. The reduction percentage of first-order vibration acceleration response peaks at three orthotropic directions are about 39 %-45 %, while they are about 75 %-85 % for the second-order. In addition, the first-order vibration acceleration response peaks at three orthotropic directions are greater than the second-order with gear tooth modification. Therefore, with the gear tooth modification, dynamic performance of the gearbox is improved significantly.

The effects of tooth modification which can be represented by the reduction of the vibration response peak are compared between the computed results and the experimental results in the Table 12. The maximum of the percentage deviation between simulated and experimental results is 11.0 %. Furthermore, through the comparison of the vibration response between the simulated results in Fig. 13 and the experimental results in Fig. 18, both the positions and the values of the typical frequencies correlate well. So, the simulated results agree well with the experimental results.

6. Conclusions

A rigid-flexible coupling model of wind turbine gearbox considering the three points mounting has been developed. An actual load spectrum was considered to perform the tooth

modification. Then the effects of the tooth modification on the dynamics were investigated. Based on the results presented, the following conclusions can be drawn.

(1) With gear tooth modification, the maximum contact pressure and face load factor are decreased. The maximum load zone on the contact pattern shifts to the center of the tooth surface, which makes the contact situation better. In addition, the peak-to-peak value of transmission error for each gear pair is reduced.

(2) The vibration response, excitations from the first-order and second-order meshing frequencies of the high-speed stage can produce a greater impact on the dynamic behaviors of the gearbox. The vibration acceleration and structural noise amplitudes at three orthotropic directions are decreased significantly within a large speed range with gear tooth modification. It indicates that gearbox dynamic performance has been improved significantly due to the gear tooth modification.

(3) An experimental real-time measurement system was developed to monitor the vibration of the wind turbine gearbox. The simulated results agree well with the experimental results.

Acknowledgment

This work was supported financially by the National Natural Science Foundation of China (No. 51575060, 51405043) and the Innovation project of the city of Chongqing (No. cstc2015zdcy-ztzx70010, cstc2015zdcy-ztzx70012).

References

[1] F. Spinato, P. J. Tavner and G. J. W. Bussel, Reliability of wind turbine subassemblies, *IET Renewable Power Generation*, 3 (4) (2009) 387-401.

[2] J. Helsen, P. Peeters and K. Vanslambrouck, The dynamic behavior induced by different wind turbine gearbox suspension methods assessed by means of the flexible multibody technique, *Renewable Energy*, 69 (3) (2014) 336-346.

[3] J. Helsen, F. Vanhollebeke and B. Marrant, Multibody modelling of varying complexity for modal behaviour analysis of wind turbine gearboxes, *Renewable Energy*, 36 (11) (2011) 3098-3113.

[4] Y. J. Park, J. G. Kim and G. H. Lee, Load sharing and distributed on the gear flank of wind turbine planetary gearbox, *J. of Mechanical Science and Technology*, 29 (1) (2015) 309-316.

[5] H. Ma, X. Pang and R. Feng, Evaluation of optimum profile modification curves of profile shifted spur gears based on vibration responses, *Mechanical Systems & Signal Processing*, 70 (2015).

[6] Z. Hu, J. Tang and J. Zhong, Effects of tooth profile modification on dynamic responses of a high speed gear-rotor-bearing system, *Mechanical Systems & Signal Processing*, 76 (2016).

[7] R. G. Parker, Dynamic modeling and analysis of tooth profile modification for multimesh gear vibration, *J. of Mechanical Design*, 130 (12) (2008).

[8] B. Yu and K. L. Ting, Compensated conjugation and gear tooth design and modification, *J. of Mechanical Design* (2015).

[9] Q. Wu, M. Feng and J. Wu, Study on contact stress of cylinder gear and tooth profile modification of offset press, *Advanced Graphic Communications, Packaging Technology and Materials*, Springer Singapore (2016).

[10] P. Velex, M. Chapron and H. Fakhfakh, On transmission errors and profile modifications minimising dynamic tooth loads in multi-mesh gears, *J. of Sound and Vibration* (2016).

[11] S. Li, Effects of misalignment error, tooth modifications and transmitted torque on tooth engagements of a pair of spur gears, *Mechanism & Machine Theory*, 83 (83) (2015) 125-136.

[12] C. Bahk and R. Parker, Analytical investigation of tooth profile modification effects on planetary gear dynamics, *Mechanism & Machine Theory*, 70 (6) (2013) 298-319.

[13] C. Zhu, X. Xu and H. Liu, Research on dynamical characteristics of wind turbine gearboxes with flexible pins, *Renewable Energy*, 68 (7) (2014) 724-732.

[14] C. Zhu, S. Chen and H. Liu, Dynamic analysis of the drive train of a wind turbine based upon the measured load spectrum, *J. of Mechanical Science and Technology*, 28 (6) (2014) 2033-2040.

[15] D. Petković, Ž. Ćojbašić and V. Nikolić, Adaptive neuro-fuzzy maximal power extraction of wind turbine withcontinuously variable transmission, *Energy*, 64 (1) (2014) 868-874.

[16] D. Petković, Ž. Ćojbašić and V. Nikolić, Adaptive neuro-fuzzy approach for wind turbine power coefficient estimation, *Renewable & Sustainable Energy Reviews*, 28 (8) (2013) 191-195.

[17] S. Shamshirband, D. Petković and H. Saboohi, Wind turbine power coefficient estimation by soft computing methodologies: Comparative study, *Energy Conversion & Management*, 81 (2) (2014) 520-526.

[18] S. Shamshirband, D. Petković and A. Amini, Support vector regression methodology for wind turbine reaction torque prediction with power-split hydrostatic continuous variable transmission, *Energy*, 67 (4) (2014) 623-630.

[19] V. Nikolić et al., Adaptive neuro-fuzzy estimation of diffuser effects on wind turbine performance, *Energy*, 89 (2015) 324-333.

[20] M. Wan, Y. Ma and J. Feng, Study of static and dynamic ploughing mechanisms by establishing generalized model with static milling forces, *International J. of Mechanical Sciences*, 114 (2016) 120-131.

[21] M. Wan, Y. Wang and W. Zhang, Prediction of chatter stability for multiple-delay milling system under different cutting force models, *International J. of Machine Tools & Manufacture*, 51 (4) (2011) 281-295.

[22] X. Jin, L. Li and W. Ju, Multibody modeling of varying complexity for dynamic analysis of large-scale wind turbines, *Renewable Energy*, 90 (2016) 336-351.

[23] H. Zhai, C. Zhu and C. Song, Influences of carrier assembly errors on the dynamic characteristics for wind turbine gearbox,

Mechanism & Machine Theory, 103 (2016) 138-147.
[24] J. Helsen, F. Vanhollebeke and F. D. Coninck, Insights in wind turbine drive train dynamics gathered by validating advanced models on a newly developed 13.2 MW dynamically controlled test-rig, *Mechatronics*, 21 (4) (2011) 737-752.
[25] O. D. Mohammed and M. Rantatalo, Dynamic response and time-frequency analysis for gear tooth crack detection, *Mechanical Systems & Signal Processing* (2015) 66.
[26] Z. Chen, W. Zhai and Y. Shao, Analytical model for mesh stiffness calculation of spur gear pair with non-uniformly distributed tooth root crack, *Engineering Failure Analysis*, 66 (2016) 502-514.
[27] ISO, *International Standard ISO 6336-1,* Second edition, 2007-04-01 (2007).
[28] SMT, *http://www.smartmt.com*.
[29] SKF, *http://www.skfcm.com*.

Shuaishuai Wang is a M.S. candidate at the State Key Laboratory of Mechanical Transmissions, Chongqing Univer- sity, China in 2015. His research area is dynamic analysis of wind turbine gearbox.

Caichao Zhu is currently a Professor at the State Key Laboratory of Mechanical Transmissions, Chongqing University, China. His research fields include the dynamics of gear systems, the tribology of mechanical transmissions, and the design of accurate transmission.